Proceedings World Geothermal Congress 2015
Melbourne, Australia, 19-25 April 2015

Finding Sufficient Permeability for Outfield Injection and Recent Drilling at Kawerau, New Zealand

John P. Clark[1], Sarah D. Milicich[2], Steven M. Sewell[1], Mohsen Askari[1] and Charis Wong[1]

[1]Mighty River Power, 283 Vaughan Road, Rotorua 3010, New Zealand

[2]GNS Science, Lower Hutt 5040, New Zealand

john.clark@mightyriver.co.nz,

Keywords: Kawerau, injection, fluid inclusions, alteration mineralogy, stratigraphy, geophysics, MT survey, thermal evolution, permeability.

ABSTRACT

Kawerau is a multi-tapper field with Mighty River Power (MRP) and Ngati Tuwharetoa Geothermal Assets (NTGA) both having to ensure they have sufficient injection to maintain operations at full capacity, as well as providing a balance between maintaining pressure support to the field and preventing thermal breakthrough to the production areas.

The Kawerau injection strategy considers a holistic reservoir view that includes numerous factors in determining the suitable locations for sustainable fluid injection. These include the proximity to the reservoir, results of geophysical resistivity surveys, the area of land available, the risk associated with the level of data known, the need to spread injection out, the position on or off suspected deep fluid pathways, and land access.

Prior to 2013, all of the deep injection at Kawerau was situated on the geophysical fringe on the northwest of the field along the direction of the regional structural trend. In order to further spread injection loads and to move injection off-strike of the regional structural trend three new deep injection wells were drilled in 2013 to the north of the field outside of the resistivity boundary zone (Allis, 1997) based on Schlumberger resistivity surveys. Two were drilled by NTGA and the third by MRP. These wells presented significant step-outs and are situated about 1.5km from the known production areas.

The injection wells encountered very good to moderate permeability with maximum temperatures of ~200˚C. Hydrothermal alteration corresponds well with more recent MT results allowing the identification of potential permeable areas outside of the previously defined field boundaries. Alteration mineralogy and fluid inclusion microthermometry from the three wells shows that in the north of the field geothermal activity was much hotter than present and that the area has undergone significant cooling. The injection wells are utilising deep permeability that had hosted past, high temperature geothermal activity.

1. INTRODUCTION

The Kawerau Geothermal Field is a high temperature geothermal field situated in the north-east of the Taupo Volcanic Zone (TVZ). The geothermal field is located within the flood plains of the Tarawera River close to the andesitic Putauaki volcano and rhyodacite domes forming the Onepu Hills. The highest measured temperatures, pressures and discharge chloride concentrations at Kawerau occur towards the southern part of the field, in the vicinity of the Putauaki volcano. This is consistent with the deep upflow and major heat source occurring in this part of the system.

Kawerau is a multi-tapper field with three companies operating on the field; Ngati Tuwharetoa Geothermal Assets Limited (NTGA), Mighty River Power (MRP) and Geothermal Developments Limited (GDL). These tappers currently have a total consented combined extraction of 159,680 tonnes of fluid per day from the geothermal field. An additional developer, Te Ahi O Maui (TAOM), was granted consent for abstraction of a further 15,000 tonnes per day in March 2014. At the time of writing this project was still under development. Injection at Kawerau began in 1991 with fluid injected in-field into shallow injection wells with total depths between -287 to -350 mRSL. In-field shallow injection continues to be carried out by NTGA into KA38, KA39 and KA40, and by GDL into GDL2 (Figure 1). MRP began deep injection into the greywacke basement in 2008 upon commissioning of their 106 MW power plant. These MRP deep injection wells (KA43, KA44, KA48, KA50, PK4, PK5 and PK8) are all located in the northeast of the field, inside or on the field reservoir boundary zone defined by Allis (1997) based on Schlumberger resistivity surveys (Figure 1). The total depths of these MRP deep injection wells are between -2085 to -2983 mRSL. In 2013, NTGA and MRP completed three new deep injection wells. The NTGA deep injection wells KA49 and KA53, and the MRP injection well KA51 are all located outside of the field reservoir boundary (Figure 1).

As a multi-tapper field, fluid injection returns are a key risk to geothermal development at Kawerau. The long-term management strategy of injection fluid for MRP and NTGA is to case injection wells deep into the greywacke basement while maintaining a one kilometre production stand-off by spreading the injection in a broad arc between one and three kilometres northwest to north-northeast of any production wells. A key aspect to the injection strategy is the need to inject fluid deep in order to prevent overloading of the shallow aquifer, while also to providing pressure support to the reservoir. Pressure support must be at a distance and depth that would prevent the cooler injection fluid returning too soon to the production area.

Geochemical monitoring and tracer testing further reinforced the need to spread injection from the northeast of the field out over a large area around the periphery of the field. This is both in case injection wells are too closely connected to the production reservoir and to avoid having large amounts of injection fluid concentrated in one place. Either of these can lead to faster injection returns and rapid cooling of production wells. The regional TVZ structural trend aligns southwest to northeast and tracer testing showed the

northeast injection area had good permeability pathways that provided connection with the production sector of the field along that strike. The spreading of injection away from the northeast moved the injection load off-strike from the production sector of the field.

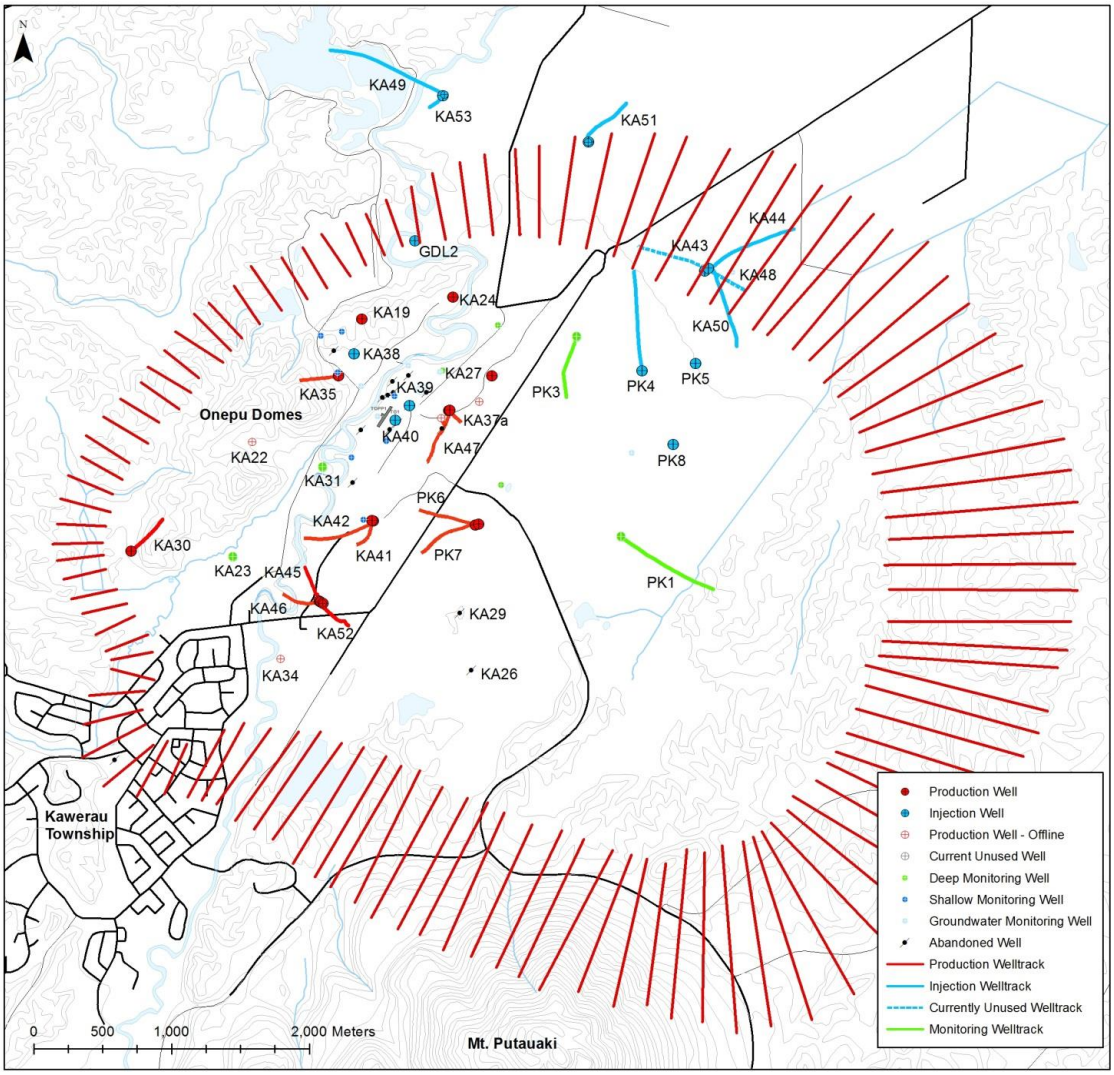

Figure 1: Location of deep injection wells including the KA49, KA51 and KA53 injection wells which are situated outside of the reservoir boundary zone (Allis 1997), which is indicated by the red shading.

2. DISCUSSION

2.2 Well Description

2.1.1 KA51 well

The well was intended to be a deep (up to 2700 mVD), inclined well drilled towards the northeast. The well is designed with the 9-5/8" production casing run to the surface. The production shoe is set about 200 m into the greywacke basement at 1566 mRSL. The well was intended to be drilled to a total depth of about -2680 mRSL. However, problems with well bore stability were encountered during drilling resulting in the drill string becoming stuck after drilling to a total depth 2209 mRSL, leaving about 500 m bottom hole assembly in the hole and ~150m of open hole beneath the production shoe. Completion testing conducted showed that KA51 has one major feedzone at -1613 to -1632 mRSL and an injectivity of about 85-115t/hr.bar. The well is capable of accepting up to ~900t/hr of fluid.

2.1.1 KA49 well

KA49 is a deviated well drilled to the northwest, about 1.5 km to the north of the nearest production well KA24 and 550 m north of the reservoir boundary zone. The well is designed with a 12-1/4" production casing and 8-1/2" slotted production liner installed in the open hole section. The well was completed to a total depth of -2248 mRSL with the production shoe set just above the greywacke basement at -1334 mRSL. Completion testing showed KA49 to have an injectivity of about 11 t/h.bar. The well has three permeable zones at -1588 to -1624 mRSL, -1669 to -1867 mRSL and -2025 to -2046 mRSL (Grant, 2013a). The bottom zone is the largest, with 60% of the total permeability, with the rest split equally between the two upper zones. Based on the completion testing the estimated injection capacity for KA49 was around 400 t/h (Grant, 2013a). The well began taking just over 400 t/hr of injection fluid from November 2013.

2.1.1 KA53 well

KA53 was drilled vertically from the same pad as KA49. The well is designed with a 12-1/4" production casing and 8-1/2" slotted production liner installed in the open hole section. The well was completed to a total depth of -2452 mRSL with the production shoe set above the greywacke basement at 1375 mRSL. Completion testing conducted in January 2013 showed KA53 to have a relatively narrow upper feedzone at -1571 to -1596 mRSL, a broader lower feedzone at -2266 to -2326 mRSL, plus a smaller feedzone near the bottom hole (Grant, 2013b). The broader lower zone has injectivity around 50 t/h.bar. The permeability of the upper zone could not be quantified. The well has been commissioned but was not being used at the time of writing.

2.2 Fluid inclusion microthermometry

In general the previous fluid inclusion homogenisation temperatures (T_h) for Kawerau obtained by Christenson (1987) and Milicich (2013) agree well with temperatures presently recorded in bores. The fluid inclusions are dominated by meteoric water with relatively low salinities (generally <5 wt. % NaCl equivalent) and show no evidence for magmatic fluid contribution (Milicich, 2013). Exceptions to this however, are distinct differences with regards to the temperatures seen in the bottom of KA16, KA24 in the northwest and KA23 in the west of the field. KA16 has seen a decrease of about 18˚C, KA24 a decrease of about 30˚C (283˚C to 250˚C) and KA23 a decrease of 20˚C since the fluids were trapped (Christenson, 1987). The fluid from KA24 is one of the most dilute, with respect to chloride indicating that the well is situated toward the margin of the system.

Simpson et al. (2013) conducted fluid inclusion microthermometry for KA49 on platy calcite crystals from -628 mRSL and -2005 mRSL. The fluid inclusions measured in the calcite crystal from -628 mRSL were primary, but the origin of inclusions in the platy calcite crystal from -2005 mRSL could not be determined. Homogenisation temperatures (T_h) for -628 mRSL ranged from 193˚C to 239˚C with a mean of 216˚C (crystal 1; Figure 2). The majority of T_h for -2005 mRL lie between 190˚C to 239˚C, with an outlier at 292˚C and a mean temperature of 221˚C (crystal 2; Figure 2). The wide range of temperatures could mean that some necked inclusions were inadvertently measured. Figure 2 compares the fluid inclusions temperatures with the heating profile for KA49 after 8 days and 31 days of heating. The fluid inclusion homogenisation temperatures at -628 mRSL depth are at least 150˚C hotter than the measured well temperatures. The fluid inclusion temperatures at -2005 mRL generally lie closer to the measured well temperatures, though are still at least 16˚C hotter than measured well temperatures. The highest temperature recorded in the well was 189˚C at -1619 mRSL which is 22˚C cooler than the mean T_h for -2005 mRSL.

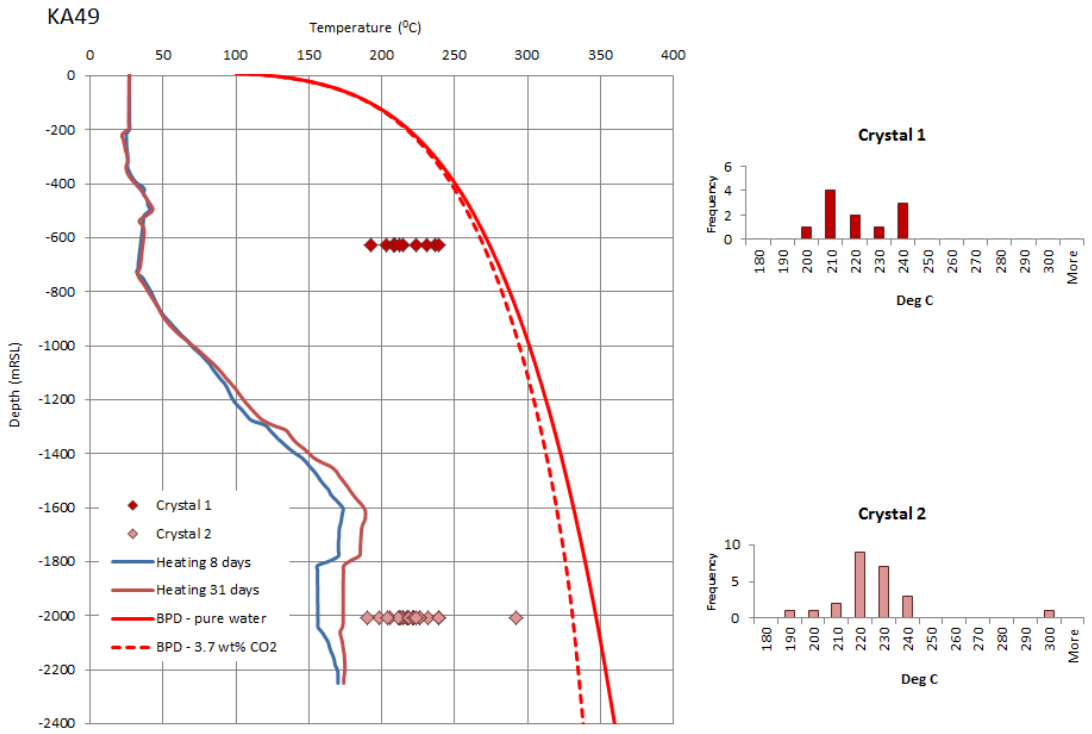

Figure 2: KA49 fluid inclusion homogenisation temperatures compared to wellbore temperature after 8 days and 31 days heating. The boiling point for depth curve (BPD) for pure water under hydrodynamic conditions and the curve for a solution containing 3.7 wt.% CO_2 are also plotted.

Sanders et al. (2013b) conducted fluid inclusion microthermometry for KA51 on two quartz crystal vein fragments from -594 mRL and two from -1014 mRL. The measured inclusions were all secondary in origin. T_h from -594 mRL for one crystal range from 171˚C to 262˚C with a mean temperature of 217˚C (crystal 1; Figure 3). The other crystal from -594 mRL had a T_h range of 160˚C to 315˚C with a mean T_h of 221˚C (crystal 2; Figure 3). One of the crystals from -1014 mRL yielded four T_h measurements. Three of these were from 310˚C to 313˚C with an outlier at 105˚C (crystal 3; Figure 3). The other crystal from -1014mRL had a T_h range of 172˚C to 345˚C with a mean temperature of 268˚C (crystal 4; Figure 3). Nine inclusions (five from KA51 and four from KA49) failed to homogenise at temperatures greater than 300 ˚C to 380˚C. Some of the higher temperatures recorded are likely due to trapping of a boiling fluid. Figure 3 compares the temperatures from the fluid inclusions with the heating profile for KA51 after 18,

25 and 34 days of heating. The fluid inclusion homogenisation temperatures measured at –594 mRSL depth are at least 140˚C hotter than the measured well temperatures. The fluid inclusion temperatures at -1014 mRSL, with the exception of one data point, are at least 60˚C hotter than the measured well temperature. One homogenisation temperature from -1014 mRSL closely matches the present day wellbore temperatures.

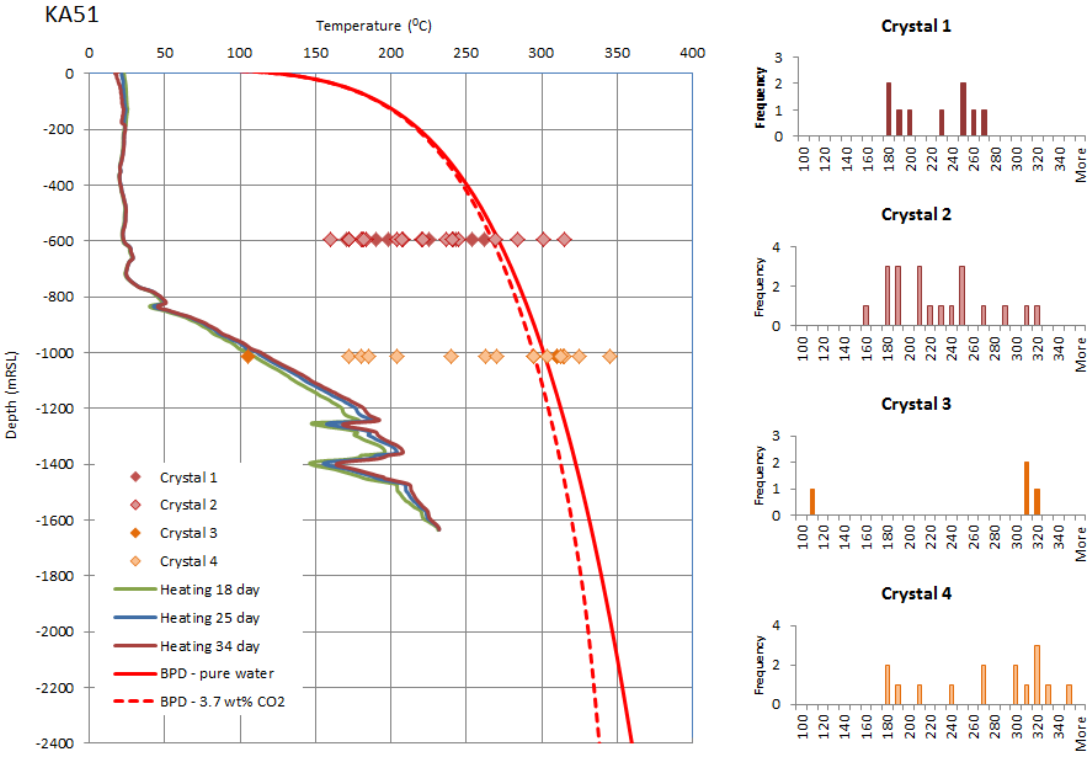

Figure 3: KA51 fluid inclusion homogenization temperatures compared to wellbore temperature after 18 days, 25 days and 34 days heating. The boiling point for depth curve (BPD) for pure water under hydrodynamic conditions and the curve for a solution containing 3.7 wt.% CO_2 are also plotted.

It is common for geothermal fluid inclusion studies of geothermal systems to have small (less than -2˚C) values for freezing point depression (Hedenquist and Henley, 1985). If the freezing point depressions (T_m) for KA49 and KA51 are solely the result of dissolved salts, then trapped fluids have an apparent salinity of 0.4 to 5.2 eq. wt.% NaCl (Figure 4). The apparent salinities were calculated using the equation from Bodnar (1993. Hedenquist and Henley (1985) showed that in the absence of CO_2 clathrates the maximum dissolved CO_2 concentration is 3.7 wt. % CO_2, which could lower the melting temperature (T_m) of pure water by up to 1.48˚C. Using the Bodnar's (1993) formula this would result in an apparent salinity of 2.54 wt. % NaCl. As no CO_2 clathrates are present in inclusions from -1014 mRSL in KA51, the T_m for the majority the inclusions requires some dissolved NaCl. A more likely explanation is that the higher wt. % NaCl values from -1014 mRSL are due to higher concentrations of CO_2 in the fluid trapped in comparison to the other crystals.

It cannot be established that the crystals formed in the same fluid event meaning it would be incorrect to assume that they represent the same fluid. The inclusions from KA51 were secondary and could represent reservoir conditions over time, though some lie across the BPD curve indicating trapping at, or close to, boiling conditions.

Assuming a fluid of low salinity was indeed boiling when some of the inclusions formed the reservoir temperature at -594 mRSL would have been ~ 225˚C to 270˚C and at –1014 mRSL ~ 280˚C to 305˚C depending upon the surface level at the time. If the palaeosurface at the time of trapping was assumed to be the Matahina ignimbrite (deposited ~ 320,000 years ago; Bailey and Carr, 1994; Leonard et al., 2010; Deering et al., 2011), the BPD curve could be depressed by up to 330 m. Figure 5 compares fluid inclusion T_h values and heating temperatures with the BPD curve for present day surface level and for the Matahina ignimbrite palaeosurface. The fluid inclusions have a wide range of T_h and relatively consistent salinities (Figure 4), indicating some formed from non-adiabatic cooling. This would support the conclusion that in the area of KA51 there has been reservoir cooling of 205˚C to 250˚C at -640mRSL and 165˚C to 190˚C at -1014mRSL.

The primary inclusions from KA49 at -628 mRSL were obtained from platy calcite which is indicative of the mineral having formed under boiling conditions (Browne, 1978, Hedenquist and Browne, 1989; Simmons and Christenson, 1994). However, T_h values for these inclusions are below the BPD curve. If the BPD curve is depressed by 330 m to a paleosurface represented by the Matahina ignimbrite, the inclusions lie close or across the BPD (Figure 5). If this is considered representative of conditions at the time fluid trapping ~ 320,000 years ago there has been about 200˚C of cooling in KA49 at -628 mRSL. The origin of the inclusions from the platy calcite crystal from -2005mRSL could not be determined though T_h are well below the BPD. This would indicate the inclusions did not trap a boiling fluid and are likely secondary, having trapped a cooler non-boiling fluid more representative of present day reservoir conditions.

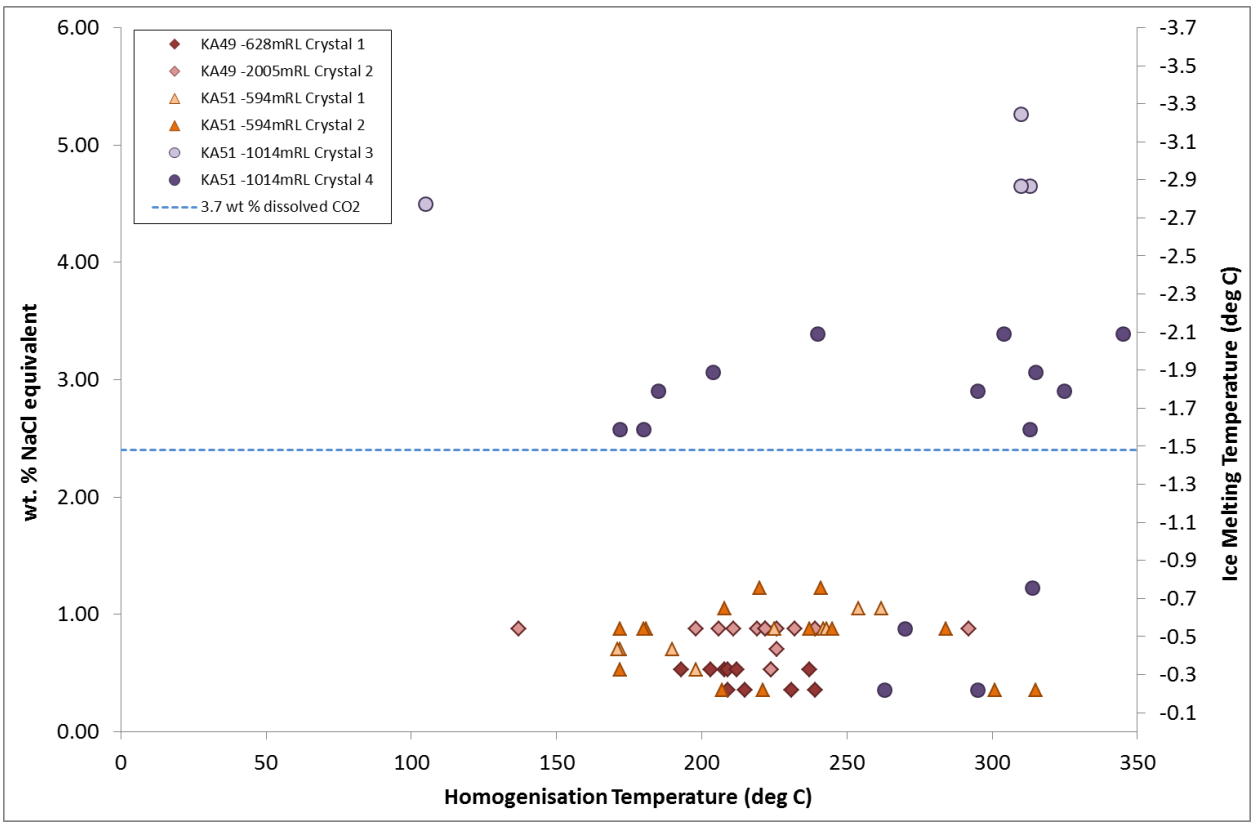

Figure 4: Bivariant plot showing measured homogenisation (T_h) and melting (T_m) temperatures with equivalent salinity (eq. wt.% NaCl).

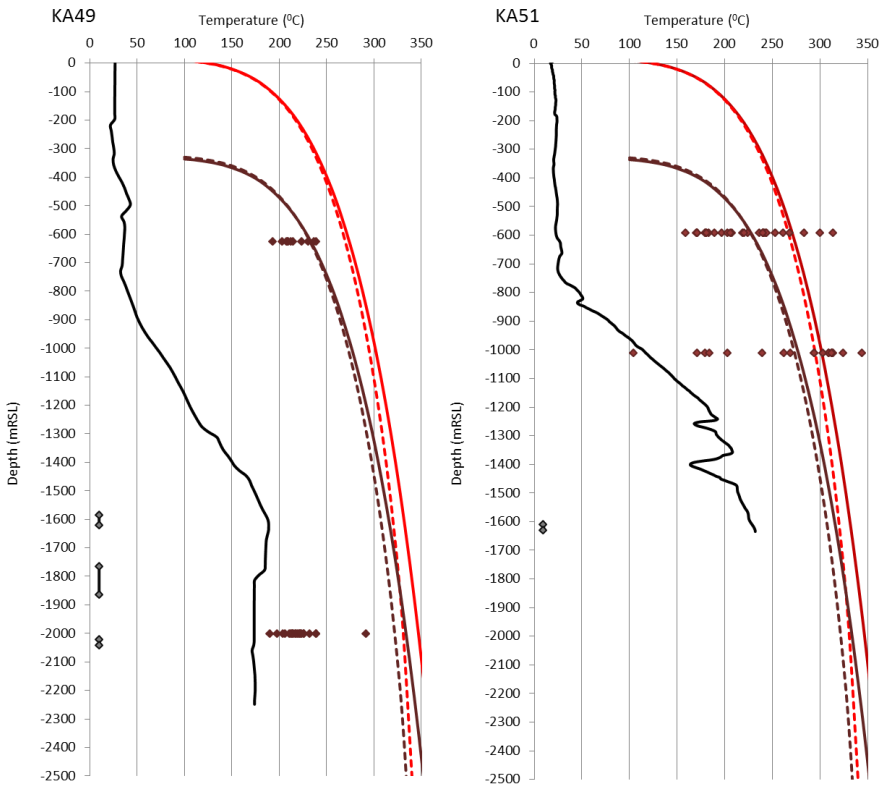

Figure 5: Fluid inclusion and heating temperatures compared to the boiling point for depth curves for pure water (solid red line) and 3.7 wt. % NaCl (dashed red line) for the present day surface and for the Matahina ignimbrite paleo-surface.

2.1 Stratigraphy and alteration mineralogy

The stratigraphy encountered by the three wells (Figure 6) is generally consistent with the stratigraphy encountered elsewhere in the field and described by Milicich et al. (2013a). In these wells the lithologically similar Raepahu and Te Teko ignimbrites were highly altered and the boundary between the two could not be determined (Sanders et al., 2013a). In KA49 a basaltic andesite not previously encountered overlies the greywacke and occurs as a dike at the bottom of the KA49 bore (Simpson et al., 2013).

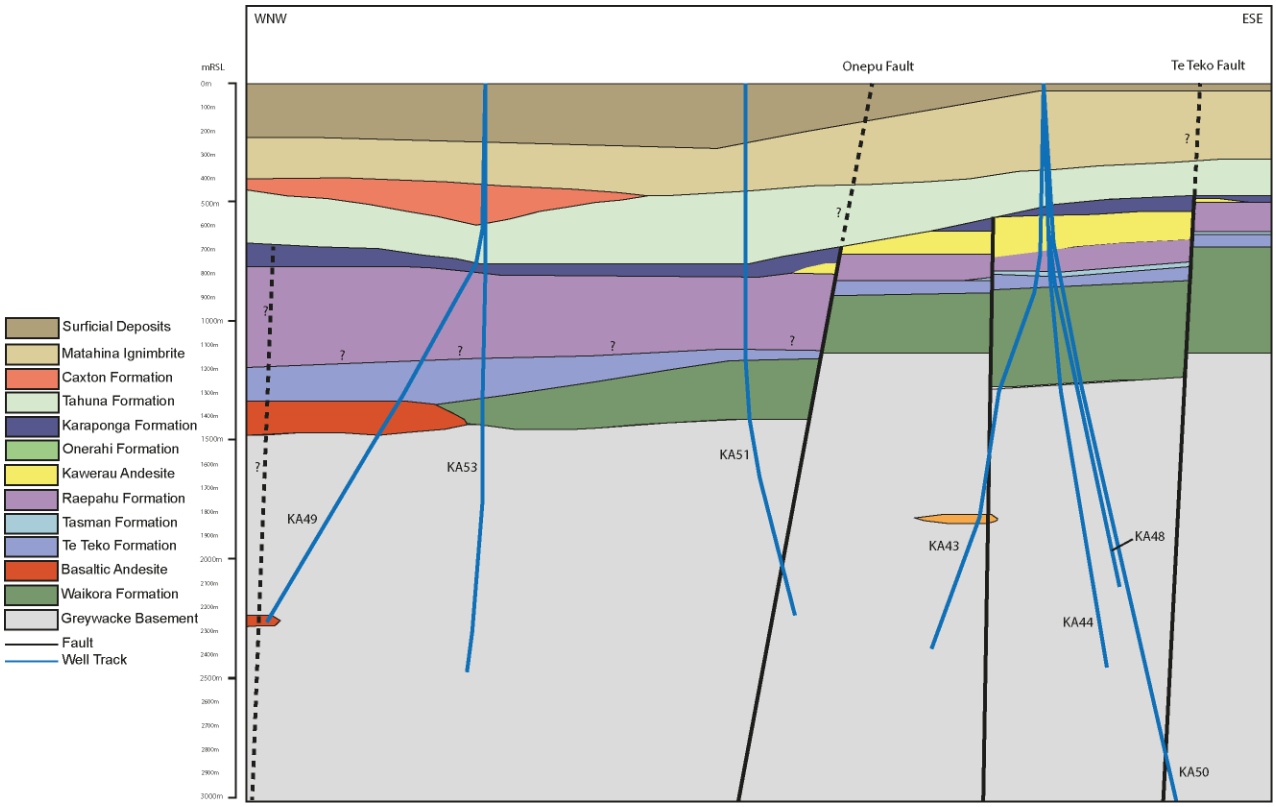

Figure 6: Stratigraphic cross-section through the northern injection wells.

The geology and alteration encountered in KA51 was described by Sanders et al. (2013). The alteration intensity in KA51 generally increases from weak to intense with depth. Smectite clay occurs around -23 m to -312 mRSL. Kaolinite occurs between -218 m to -328 mRSL. Interlayered illite-smectite occurs from around -328 m to -423 mRSL, with crystalline illite occurring from -423 mRSL. Epidote occurs between -428 m to 443 mRSL, again between -478 m to -493 mRSL, and consistently below -1320 mRSL. Chlorite occurs with smectite in the surficial deposits, and with illite in the Raepahu/Te Teko formations, Waikora Formation and the greywacke basement. Calcite and quartz-pyrite veins are common from -895 mRSL. Figure 7 compares the occurrence and general stability ranges for selected hydrothermal minerals with the heating profiles obtained from the KA51. The hydrothermal mineral distribution indicates prograde temperatures with depth. The temperature profile for the well after 34 days heating is generally lower than the hydrothermal mineral stability ranges, particularly between -328 m to -1230 mRSL. Temperatures in KA51 are consistently over 200˚C below -1455 mRSL. Similar temperatures were observed in KA43 and KA44 injection wells in the northeast of the field. Fluid inclusion T_h generally agree well with the hydrothermal mineral stability ranges.

The geology and alteration encountered in KA49 was described by Simpson et al. (2013). In KA49 most units are moderately to strongly altered, with the Raepahu/Te Teko formations and greywacke intensely altered. The basaltic andesite encountered overlying the greywacke is weakly altered, except for the top and base which is strongly altered. No cuttings were obtained until -202 mRSL, where the alteration minerals smectite and kaolinite occur until -312 mRSL. Interlayered illite-smectite occurs from -317 m to -747 mRSL. Illite occurs from -765 mRSL. Rare to minor epidote occurs in the basaltic andesite and greywacke below -1413 mRSL. Actinolite occurs at -1416 mRSL and -2230 mRSL within with the basaltic andesite. Beneath the Matahina ignimbrite, from -437 mRSL, quartz and pyrite are pervasive, and calcite is common. Albite and adularia replacing primary plagioclase is found at -773 mRSL, -1002 mRSL and -1315 mRSL. Actinolite occurs in the basaltic andesite at -1416 mRSL and -2233 mRSL. Prehnite occurs intergrown with epidote at -1990 mRSL. Quartz and pyrite occur throughout the well and calcite occurs from -452 mRSL. Platy calcite is sporadically found in minor quantities from -1481 m to -1515 mRSL, -1707 m to -1867 mRSL, -1954 m to -1990 mRSL, and more commonly found from -2112 m to -2129 mRSL and below -2216 mRSL. Chlorite occurs in the Caxton Formation, but is consistently found in the basaltic andesite and the greywacke basement. Figure 8 compares the occurrence and general stability ranges for selected hydrothermal minerals with the 31 day heating profile obtained for the well. The distribution of hydrothermal minerals indicates prograde temperatures with depth. The temperature profile for the well after 31 days heating is generally lower than the hydrothermal mineral stability ranges. The highest temperature recorded in the well is 189˚C at -1619 mRSL. Fluid inclusion T_h obtained at -628 mRSL lie at the upper end, or higher, of the stability range for interlayered illite-smectite. T_h from -2005 mRSL, with the exception of one outlier, are below the stability range for epidote, indicating the inclusions represent a fluid cooler than those that formed the epidote present at this depth, and this part of the reservoir has undergone cooling.

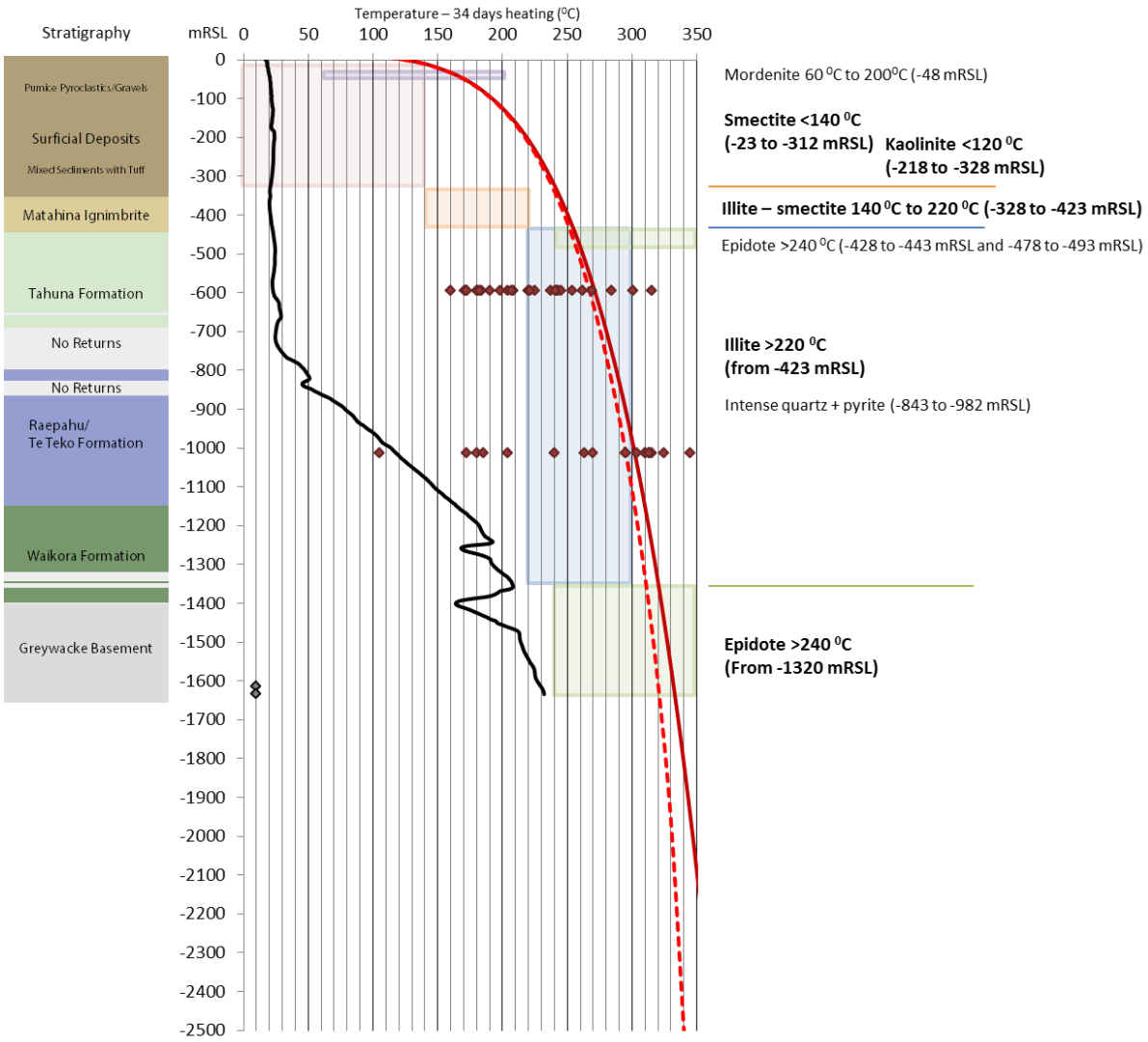

Figure 7: KA51 - Occurrence and general stability ranges (from Reyes, 1998 and Browne, 1978) for selected hydrothermal minerals compared to the 34 day heating profile (black line) obtained for the well. The stratigraphy is shown to the left of the graph, fluid inclusion T_h are shown by the dark red diamonds. The boiling point for depth curve (BPD) for pure water under hydrodynamic conditions is shown by the solid red line and the curve for a solution containing 3.7 wt.% CO_2 is shown by the dashed red line. Feedzones are indicated by the grey diamonds near the y-axis.

The geology and alteration encountered in KA53 was described by Simpson and Rae (2013). In KA53 the alteration intensity is weak in the volcaniclastic sediments of the surficial deposits. The underlying units are generally strongly altered, with the Raepahu/Te Teko and Rotoroa formations being intensely altered. Kaolinite and intermittent smectite occur in the surficial deposits between -136 m to -311 mRSL. Interlayered illite-smectite occurs between -316 m to -376 mRSL and illite from -376m to -471 mRSL. Smectite occurs again between -471m to -776 mRSL in the Caxton Rhyolite and the Tahuna Formation, with mordenite occurring at -576 mRSL. Illite occurs consistently from -776 mRSL and epidote occurs with chlorite from -1266 mRSL. Quartz and pyrite occur throughout the well and calcite common is common from -431 mRSL. Rare platy calcite is found at -1651 mRSL, -1706 mRSL, -1726 mRSL and -1746 mRSL. Chlorite occurs from -1246 mRSL in the Raepahu/Te Tekoand Waikora formations and greywacke basement. Figure 9 compares the occurrence and general stability ranges for selected hydrothermal minerals with the heating profiles obtained from the well. The distribution of hydrothermal minerals indicates prograde temperatures with depth, with a temperature inversion occurring between -471 m and -776 mRSL. The temperature profile for the well after 1 day heating is generally lower than the hydrothermal mineral stability ranges, particularly between -316 m to -1345 mRSL. KA53 has temperatures just over 200˚C in the open hole section between -1576 m and -1716 mRSL.

2.2 Magnotellurics (MT)

Similar to other geothermal fields the low resistivity (or high conductance) at Kawerau corresponds to hydrothermal alteration clay with low permeability that forms over and adjacent to the higher temperature and more permeable reservoir rock. Electrically conductive clays (i.e. smectite), formed by geothermal fluid altering the rock above the reservoir, are imaged as low resistivity by the MT. These smectite clays tend to form at temperatures <140 ˚C, but can occur up to ~200˚C (Simmons et al., 1992), and generally form an impermeable clay cap and margin to the more resistive permeable geothermal system. The distribution and intensity of low resistivity smectite clay alteration can provide a general guide to the overall pattern of permeability in the underlying, higher resistivity, higher temperature reservoir.

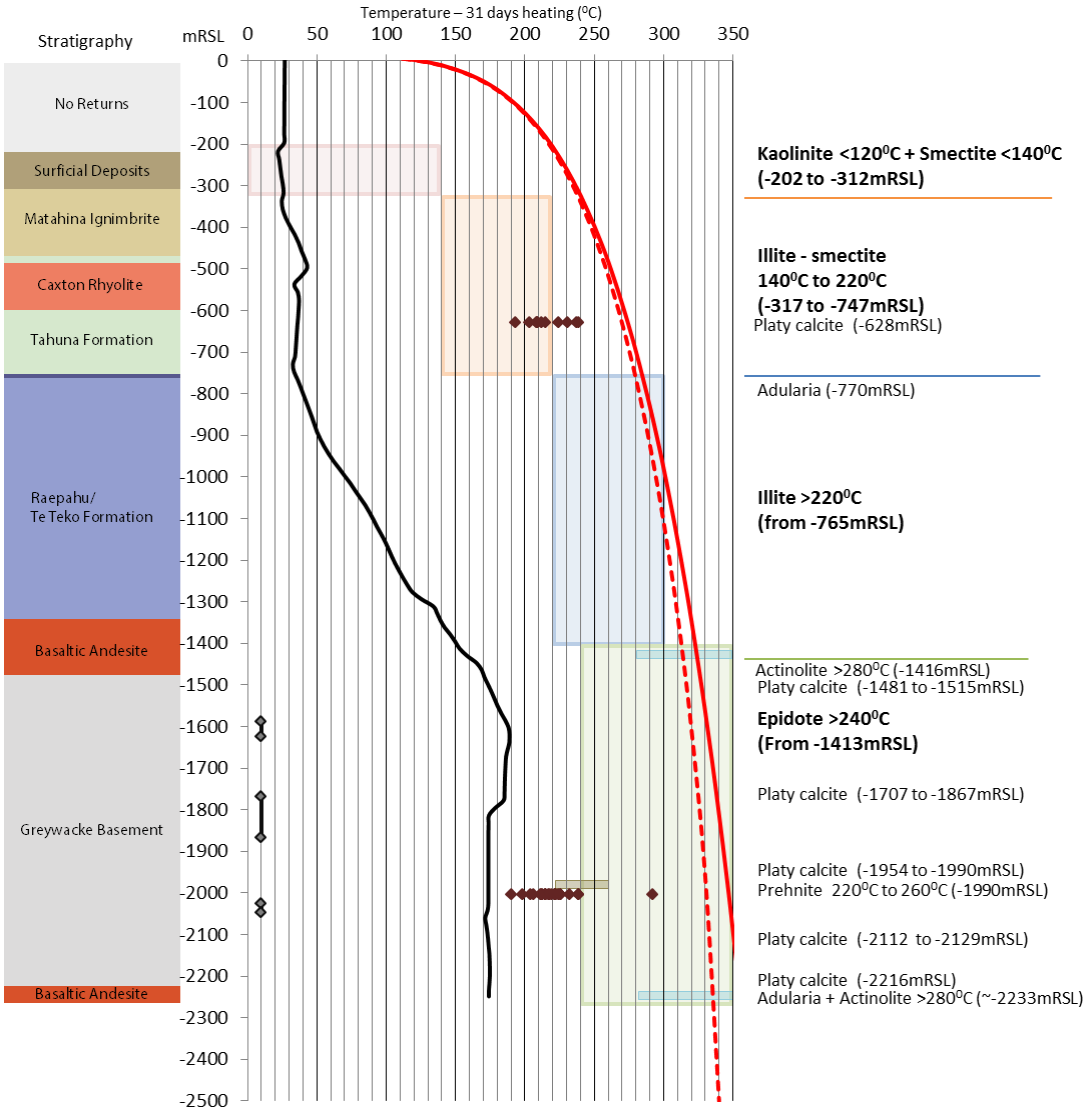

Figure 8: KA49 - Occurrence and general stability ranges (from Reyes, 1998 and Browne, 1978) for selected hydrothermal minerals compared to the 31 day heating profile (black line) obtained for the well. The stratigraphy is shown to the left of the graph, fluid inclusion T_h are shown by the dark red diamonds. The boiling point for depth curve (BPD) for pure water under hydrodynamic conditions is shown by the solid red line and the curve for a solution containing 3.7 wt.% CO_2 is shown by the dashed red line. Feedzones are indicated by the grey diamonds near the y-axis..

Based on previous MT surveys Cumming (2009) identified a geophysical field boundary which corresponds to a very thin conductive clay cap and underlying resistive reservoir. Beyond this was an intermediate zone which corresponds to a sloping or irregular zone between the very shallow cap and deep clay alteration and then an outer zone of deep alteration associated with thick, tabular clay alteration that could be associated with deep, high temperature but generally lower permeability. KA51 is situated on the boundary of the intermediate zone and drilled into the outer zone. KA49 and KA53 are situated in the outer zone of deep alteration.

A further MT survey was conducted by MRP in November 2012 partly in order to build a more robust data set and reduce the risk and potentially the cost associated with drilling new injection wells targeted at the edge of the field, particularly in the north. Figure 10 shows an MT resistivity cross-section from the 2012 3D inversion through the north of the field aligned WNW to ESE between KA49 in the west and KA50 in the east. The survey showed that to the north of the field in the area of the three new injection wells the clay cap is thick in the northeast injection area (KA50) with the base lying at around -1500 mRSL. The base of the clay cap is significantly shallower and higher resistivity in the KA51 area at about -450 mRSL elevation, and it deepens again towards KA53 where it is about -750 mRSL deep and continues to deepen towards the west to about -1200m elevation beyond KA49. This interpretation is consistent with the methylene blue results from the three wells (Figure 10). Based on present day well temperatures, the MT data also suggest that the reservoir has been hotter in the past in the area of KA51 and KA53. The structure of the clay cap through this region is consistent with the KA51-KA53_KA49 area having hosted a fossil hydrothermal system, proximal, but not contemporaneous with the present day system. Present day temperatures from surface to approximately -800 m elevation in KA51, KA49 and KA53 are isothermal and ~50 ˚C indicating that the smectite zone no longer acts to cap the system in this area. The recent MT results show an area centred around KA51 where a previous high temperature geothermal system has resulted in a relatively thin, clay cap beneath which there is good probability of finding sufficiently high permeability for injection.

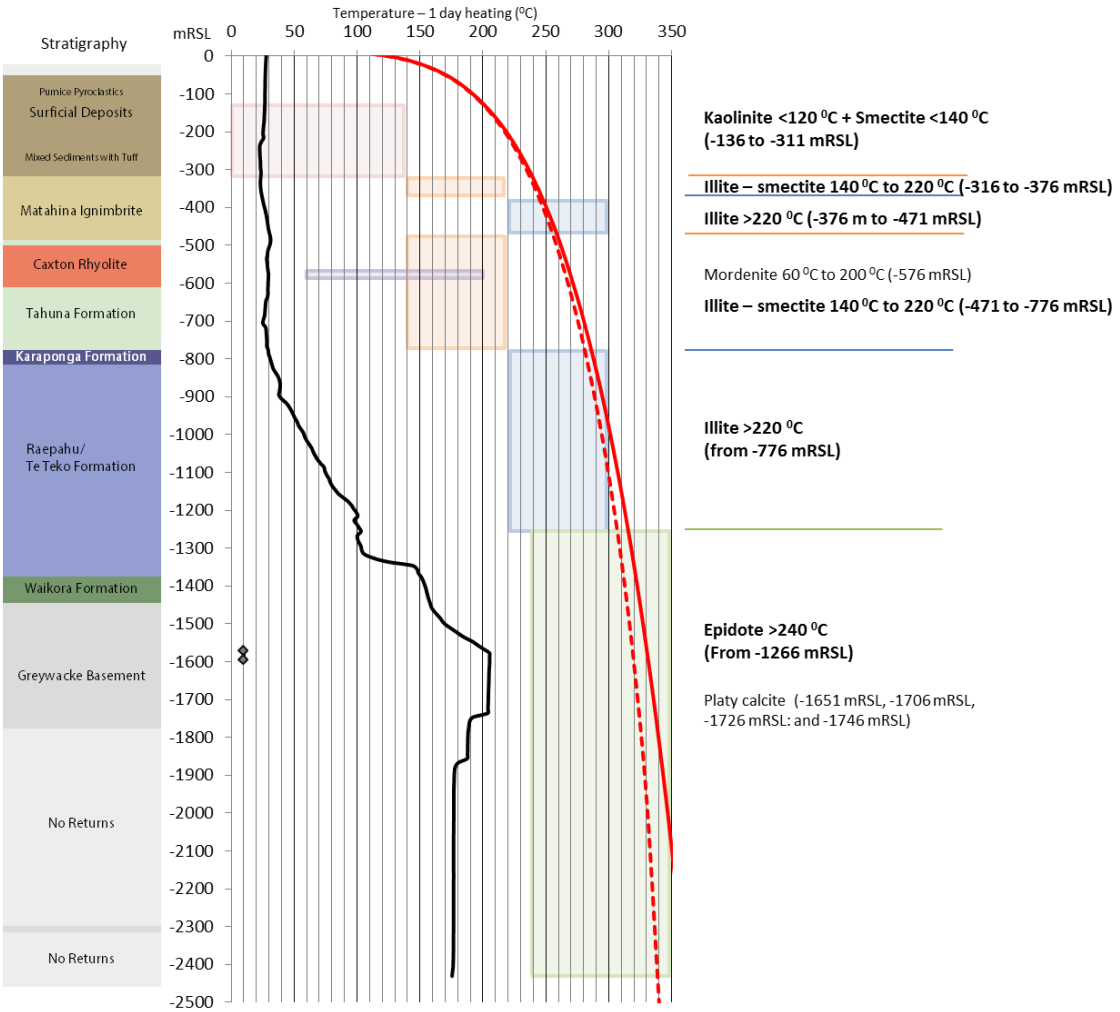

Figure 9: KA53 Occurrence and general stability ranges (from Reyes, 1998 and Browne, 1978) for selected hydrothermal minerals compared to the 1 day heating profile (black line) obtained for the well. The stratigraphy is shown to the left of the graph, fluid inclusion T_h are shown by the dark red diamonds. The boiling point for depth curve (BPD) for pure water under hydrodynamic conditions is shown by the solid red line and the curve for a solution containing 3.7 wt.% CO_2 is shown by the dashed red line. Feedzones are indicated by the grey diamonds near the y-axis.

2.3 Thermal Evolution

Milicich et al. (2013) found there are four known periods where magma has been present beneath the Kawerau area that could have provided a heat source for a local hydrothermal system. These have been dated as follows:

0.60 and 1.0 Ma	Kawerau Andesite (Milicich et al., 2013b)
0.36 Ma and 0.43 Ma	Caxton Formation rhyolite lavas and intrusions and slightly older locally source tuffs of the Tahuna Formation (Milicich et al., 2013b)
150 ka	Onepu Formation extrusive domes and intrusives (Milicich et al., 2013b)
2400 and 8350 years	Mt Putauaki andesite-dacite domes (Carrol et al. 1997)

Milicich et al. (2014) found that of these identified episodes of local magmatism, only those associated with the latest Quaternary Putauaki and the 0.43–0.36 Ma Tahuna/Caxton formations are likely to have provided a heat source for a hydrothermal system. However, periods of thermal activity at Kawerau could be related to magma not yet encountered by drilling or to the emplacement of magmatic intrusions at depths greater than that encountered by drilling that may not have any related surface expression.

However, two of these periods identified by Milicich are associated with hydrothermal eruption breccias. The oldest was identified from core in KA25 below the 360,000 year old Caxton Formation (Milicich et al., 2013a). The youngest hydrothermal eruption breccias were mapped at surface by Nairn and Wiradiradja (1980) and associated with an eruption crater to the east of KA26. These two younger eruption breccias were constrained by tephra ages at around 16,000 years ago and 9,000 years ago (Lowe et al., 2013).

Milicich (2013) found overprinting of high-temperature alteration with low-temperature is characteristic of the north of the field. This is further supported by the results from the KA51, KA49 and KA53 wells. Fluid microthermometry suggests that some

inclusions could have trapped fluid representing conditions of a hydrothermal system that existed at Kawerau over 330,000 years ago. Alteration mineralogy and fluid inclusion microthermometry from the KA51, KA49 and KA53 wells shows that to the north of the field geothermal activity has been much hotter than current conditions and the area has undergone significant cooling.

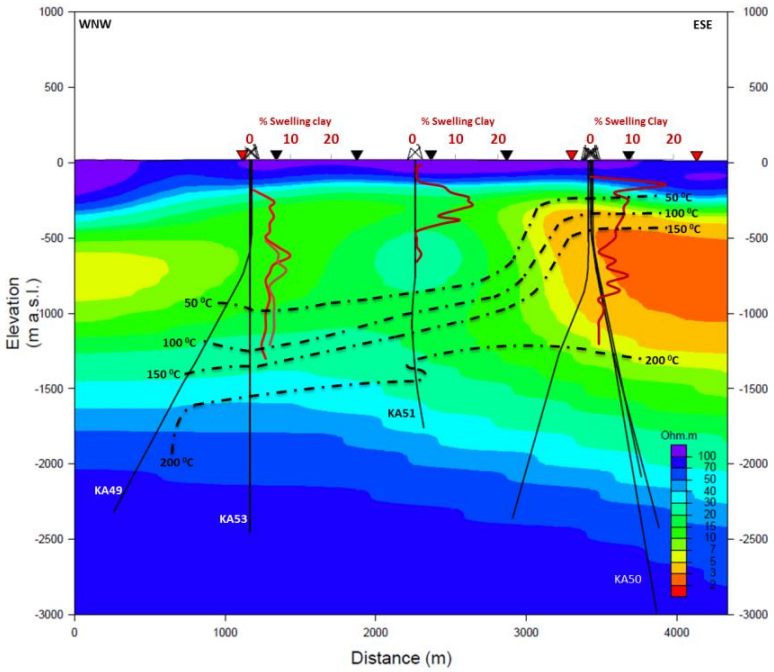

Figure 10: An MT resistivity cross-section from the 2012 3D inversion through the north of the field between KA49 in the west and KA50 in the east. The percentage swelling clay based on MeB results for KA50, KA51 and K49 are shown by the red lines; KA53 is shown by the dark red line. Note that there is no data above -536 mRSL for KA53.

Christenson (1987) suggested there had been a shift in heat source away from the north-west Onepu Ridge area to the southeast associated with Mt. Putauaki intrusives. Milicich et al. (2014) suggests the Kawerau hydrothermal system has been made up of two overprinted hydrothermal systems since approximately 400,000 years B.P. It is not known whether hydrothermal activity was continuous or intermittent between the earlier system associated with the Caxton Formation and the current system associated with Mt. Putauaki magmatics. However, the three new injection wells situated to the north of the field appear to utilise permeability that had hosted past thermal activity likely associated with the older Kawerau hydrothermal system. Understanding the thermal evolution of hydrothermal system and the use of MT to help develop conceptual elements can be useful in identifying areas that have hosted past geothermal activity which may provide sufficient permeability for outfield injection.

3.0 CONCLUSION

As Kawerau is a multi-tapper field it is highly important that in determining suitable locations for sustainable fluid injection a holistic reservoir view is used that takes into account numerous factors such as:

- Proximity to the reservoir
- Results of geophysical resistivity surveys
- Risk associated with the level of data known
- Need to spread injection out, the position on or off suspected deep fluid pathways
- The area of land available, and access arrangements to that land

Prior to 2013, all of the deep injection at Kawerau was situated in the northwest of the field inside the resistivity boundary zone identified by Allis (1997) based on Schlumberger resistivity surveys. The use of this holistic approach was critical in identifying other suitable locations for future injection and significantly reduced the risk associated with step-out outfield drilling. The assessment of known information and conducting further geophysical surveys allowed for the identification of areas that have hosted past geothermal activity that would likely provide permeability for outfield injection. This resulted in the three new injection wells drilled by MRP and NTGA in 2013 finding sufficient injection to allow the two companies to maintain operations at full capacity.

ACKNOWLEDGEMENT

Authors are appreciative of, and wish to thank, the management of Mighty River Power and Ngati Tuwharetoa Geothermal Assets for their permission to publish this paper and all staff who have provided inputs and helped complete this work. Authors would also like to thank GNS for their work carried out during well drilling.

REFERENCES

Allis, R.G.: The natural state and response to development of the Kawerau geothermal field, New Zealand. *Geothermal Resource Council Transactions*, **21**, (1997), 3-10.

Bailey, R.A., and Carr, R.G.: Physical geology and eruptive history of the Matahina Ignimbrite, Taupo Volcanic Zone, North Island, New Zealand. *New Zealand Journal of Geology and Geophysics*, **37**, (1994), 319-344.

Bodnar, R.J.: Revised equation and table for determining the freezing point depression of H2O-NaCl solutions. *Geochemica et Cosmochimica Acta*, **57**, (1993), 683-684.

Browne, P.R.L.: Hydrothermal alteration in active geothermal fields. *Annual Review of Earth and Planetary Science*, **6**, (1978), 229-250.

Carroll, L.D., J.A. Gamble, B.F. Houghton, T. Thordarson, and T.F.G. Higham, 1997. A radiocarbon age determination for Mount Edgecumbe (Putauaki) volcano, Bay of Plenty, New Zealand. *New Zealand Journal of Geology and Geophysics*, **40**, (1997), 559-562.

Christenson, B.W.: Fluid-Mineral Equilibria in the Kawerau Hydrothermal System, Taupo Volcanic Zone, New Zealand. PhD (Geology) thesis, University of Auckland, (1987).

Cumming, W.B.: Kawerau conceptual model from MT for injection targeting. Internal MRP Report. (2009).

Deering, C.D., Cole, J.W., and Vogel, T.A.: Extraction of crystal-poor rhyolite from a hornblende-bearing intermediate mush: a case study of the caldera-forming Matahina eruption, Okataina volcanic complex. *Contributions to Mineralogy and Petrology*, **161**, (2011), 129-151.

Grant, M.A.: KA49 Completion test. MAGAK report to NTGA. (2013a).

Grant, M.A.: KA53 Completion. MAGAK Report to NTGA. (2013b).

Hedenquist, J.W., and Browne, P.R.L.: The evolution of the Waiotapu geothermal system, New Zealand, based on the chemical and isotopic composition of its fluids, minerals, and rocks. *Geochimica et Cosmochimica Acta*, **53**, (1989), 2235-2257.

Hedenquist, J.W., and Henley, R.W.: The importance of CO2 on freezing point measurements of fluid inclusions: Evidence from active geothermal systems and implications for epithermal ore deposits. *Economic Geology*, **80**, (1985), 1379-1406

Leonard, G.S., Begg, J.G., and Wilson, C.J.N. (compilers): Geology of the Rotorua area: scale 1:250,000. Institute of Geological & Nuclear Sciences 1:250,000 geological map 5. Institute of Geological & Nuclear Sciences Limited, Lower Hutt, New Zealand, (2010).

Lowe, D.J., M. Blaauw, A.G. Hogg, and R.M. Newnham: Ages of 24 widespread tephras erupted since 30,000 years ago in New Zealand, with re-evaluation of the timing and palaeoclimatic implications of the Late glacial cool episode recorded at Kaipo bog. *Quaternary Science Reviews*, **74**, (2013), 170-194.

Milicich, S.D.: Aspects of the Chronology, Structure and Thermal History of the Kawerau Geothermal Field. PhD thesis, Victoria University of Wellington, New Zealand. http://researcharchive.vuw.ac.nz/handle/10063/3044, (2013).

Milicich, S.D., Wilson, C.J.N, Bignall, G., Pezaro, B. and Bardsley, C.: Reconstructing the geological and structural history of an active geothermal field: a case study from New Zealand. *Journal of Volcanology and Geothermal Research*, **262**, (2013a), 7-24.

Milicich, S.D., Wilson, C.J.N., Bignall, G., Pezaro, B., Charlier, B.L.A., Wooden, J.L., and Ireland, T.R.: U-Pb dating of zircon in hydrothermally altered rocks of the Kawerau Geothermal Field, Taupo Volcanic Zone, New Zealand. *Journal of Volcanology and Geothermal Research*, **253**, (2013b), 97-113.

Milicich, S.D., Chambefort, I., Bignall, G., and Clark, J.: Overprinting hydrothermal systems in the Taupo Volcanic Zone. *Geothermal Resources Council Transactions*, In Press (2014).

Nairn, I.A., Wiradiradja, S.: Late Quaternary hydrothermal explosion breccias at Kawerau Geothermal Field, *New Zealand. Bulletin Volcanologique*, **43**, (1980), 1-13.

Reyes, A.G., 1998. Petrology and Mineral Alteration in Hydrothermal Systems: From Diagenesis to Volcanic Catastrophes. United Nations University Geothermal Training Programme, Iceland, Report No. 18. 77pp.

Sanders, F., Lewis, B., Simpson, M.P., and Milicich, S.D.: Geology of Well KA51, Kawerau Geothermal Field. GNS Science Consultancy Report 2013/228. (2013a).

Sanders, F., Milicich, S.D., and Rae, A.J.: Results of Fluid Inclusion Microthermometric Measurements of Quartz Vein Fragments from KA51, Kawerau Geothermal Field. GNS Letter Report No. CR2013/323 LR. 9p. (2013b)

Simmons, S.F., Browne, P.R.L., and Braithwaite, R.L.: Active and extinct hydrothermal systems of North Island, New Zealand. *Society of Economic Geologists*. **15**, (1992).

Simmons, S.F., and Christenson, B.W.: Origins of calcite in a boiling geothermal system. *American Journal of Science*, **294**, (1994), 361-400.

Simpson, M.P., Massiot, C., and Rae, A.J.: Geology of Well KA49, Kawerau Geothermal Field. GNS Science Consultancy Report 2013/50. 51p. (2013)

Simpson, M.P., and Rae, A.J.: Geology of well KA53, Kawerau Geothermal Field. GNS Science Consultancy Report 2013/56. (2013)